

# A Structural Analysis of Column Gusset Plates on the Production Module Support Structures

**Andi Ardianti**

Department of Naval Architecture, Hasanuddin University, Makassar, Indonesia  
aardianti@gmail.com (corresponding author)

**Muhammad Najib Sadikin Daerobi**

Department of Naval Architecture, Hasanuddin University, Makassar, Indonesia  
smuh.najib@gmail.com

**Muhammad Zubair Muis Alie**

Department of Ocean Engineering, Hasanuddin University, Makassar, Indonesia  
zubair.m@eng.unhas.ac.id

Received: 2 December 2025 | Revised: 20 January 2026 | Accepted: 28 January 2026

Licensed under a CC-BY 4.0 license | Copyright (c) by the authors | DOI: <https://doi.org/10.48084/etasr.16645>

## ABSTRACT

Floating Production Storage and Offloading (FPSO) units are complex offshore production facilities, whose topside modules are supported by multicolumn structures. A main component of this system is the gusset plate, which connects and reinforces the joints between the columns and other structural members while distributing internal forces. Under combined static and dynamic loading, gusset plates are prone to localized deformation, which may reduce joint stiffness and compromise structural stability. This study analyzes the mechanical behavior of the gusset plates in production module support structures using numerical analysis based on the Finite Element Method (FEM). Three different gusset plate configurations were developed and compared to evaluate the influence of geometry on the stress distribution, deformation patterns, and safety factors under identical operational and environmental load cases. The results indicate that gusset geometry significantly affects stress concentration, with the Corner model exhibiting the highest Von Mises stress (647 MPa), the Round model showing moderate improvement (567 MPa), and the Flat model achieving the lowest stress (474 MPa) and the most uniform distribution. These findings highlight the importance of geometric optimization in enhancing the structural reliability and load-transfer performance of production-module support systems.

*Keywords-topside module; supporting column; gusset plate; finite element method*

## I. INTRODUCTION

Floating Production Storage and Offloading (FPSO) units are widely used in offshore oil and gas operations due to their high storage capacity, flexibility, and ability to operate in deepwater fields [1]. An FPSO receives hydrocarbons from subsea wells, processes them, and stores stabilized crude oil before offloading it to shuttle tankers, making it a key facility in modern offshore development. The topside of an FPSO comprises multiple modules that accommodate processing and utility systems supported by multicolumn structural frameworks [2, 3]. Ensuring the integrity of these structural supports is crucial for the safe and reliable long-term operation of FPSOs. A significant element in the topside supporting framework is the gusset plate, which connects and reinforces the joints between the columns, beams, and deck members [4, 5]. Gusset plates help transfer and redistribute forces across the structural system, thereby improving joint stiffness and local stability. However, FPSOs operate under combined static and

dynamic loading, including equipment weight, environmental forces, and vessel motion due to waves and wind [6, 7]. These conditions may lead to stress concentration and localized deformation in gusset plates, compromising load distribution and reducing overall structural reliability [4, 8].

The global structural response of FPSO modules has been examined using Finite Element Analysis (FEA) [2, 9]. Specific aspects, such as fire response [1], buckling behavior [10, 11], and optimization of topside module configurations, have also been addressed [9]. Finite element investigations, including analyses of double beams connected by elastic springs and steel-concrete composite plates, have demonstrated that joint stiffness and plate interaction significantly influence overall structural performance [12]. Similarly, studies on beams with elastic connections and steel-composite plates have shown that connection behavior and plate-bar interaction affect stiffness characteristics and critical buckling loads. In addition, limit-load analyses of bending plates have provided further insights

into failure mechanisms in plate-based structural systems [13]. The existing literature mainly focuses on global structural behavior and large-scale members. Limited attention has been given to the localized stress and deformation behavior of gusset plates, even though they play a significant role in load transfer and joint stability. Consequently, a dedicated investigation of the localized structural response of gusset plates is necessary to improve connection reliability and optimize their design in FPSO support structures. The structural integrity of production modules is governed by the strength and stability of their supporting frameworks, particularly at the beam-column connections. Gusset plates are crucial components within these joints, as they facilitate load transfer between members while increasing joint stiffness and overall structural stability. Inadequate gusset plate design can result in stress concentration, localized deformation, and even premature failure, thereby reducing the reliability of the entire support system. The geometry and configuration of gusset plates significantly influence the strength and performance of structural connections [14]. Stress analyses have further indicated that, although general distribution patterns may appear consistent across different connection types, specific regions of the gusset plate are prone to elevated stress levels and require careful design consideration [8]. These findings underscore the importance of optimizing gusset plate geometry to enhance connection performance in production module support structures.

Damage at the interface of structural joints can lead to progressive degradation of the bonding region, ultimately resulting in structural failure. Such damage typically initiates at the loaded end and propagates along the interface, potentially triggering global collapse if not properly addressed [15]. To evaluate and predict this behavior, FEA is employed to model steel structural connections, including gusset plates, supporting columns, and topside module frameworks, allowing accurate assessment of stress distribution, strength, and overall structural response [16]. Research on the net-section fracture resistance of gusset plates with various connection details has indicated that conventional design approaches, such as the Whitmore method, may underestimate the actual load-carrying capacity, particularly in non-seismic connections with welded edges [17]. In production module support structures, gusset plates are installed at column connections to enhance joint stiffness and strength, enabling the system to resist combined axial and shear forces effectively [18]. Furthermore, advanced numerical approaches, including thermo-mechanical analyses, enable detailed prediction of residual stresses, temperature gradients, and deformation behavior in welded or mechanically joined structures [19]. Such methods provide greater insights into connection performance and structural integrity under complex loading conditions [20]. Despite these advances, limited research has focused specifically on the localized stress and deformation behavior of the gusset plates within FPSO production module supports. Therefore, this study addresses this gap by conducting a finite element-based numerical investigation of three different gusset plate configurations. The objective is to systematically evaluate and compare their stress distribution, deformation characteristics, and safety factors under identical loading and boundary conditions.

## II. METHODOLOGY

This study adopts a numerical methodology based on FEM to evaluate the structural behavior of gusset plates in FPSO topside module support systems. The research procedure includes geometric model development, definition of loading scenarios and boundary conditions, finite element discretization, and subsequent assessment of stress and deformation responses.

### A. Production Module Data

The production module model and its dimensions are shown in Figure 1 and Table I, respectively.

TABLE I. MAIN DIMENSIONS OF PRODUCTION MODULE

Dimensions	Value (m)
Height	29.7
Length	29.7
Width	27

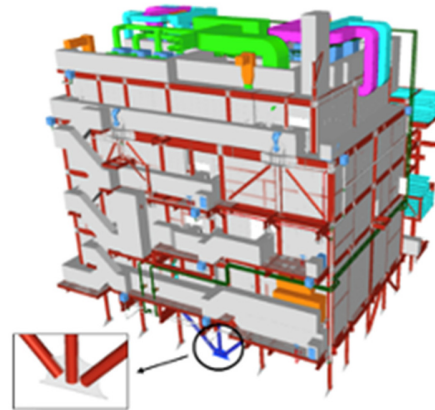


Fig. 1. Model of the production module.

### B. Model Development

Three different gusset plate configurations were developed to evaluate their structural performance under identical loading and boundary conditions. Each model represented a typical connection between vertical and inclined columns in a production module support structure, with variations in the gusset plate geometry and stiffening layout. The gusset plates were modeled with a thickness of 37.5 mm, and the column members were modeled as hollow circular pipes with a wall thickness of 20 mm. These dimensions were selected to represent realistic offshore structural proportions commonly used in production-module frameworks. Fixed supports were applied along the lower edge of the gusset plate to simulate a rigid connection with the supporting structure. The three gusset plate configurations developed for comparison in this study are shown in Figure 2.

### C. Material Properties

The structural components of the production module, including the gusset plates and supporting members, are made of marine-grade steel type AH/DH36, which is used in offshore and ship structures, due to its high yield strength and good toughness. The material was assumed to behave isotropically

and linearly elastically within the elastic limit. The mechanical properties of the gusset plate are listed in Table II.

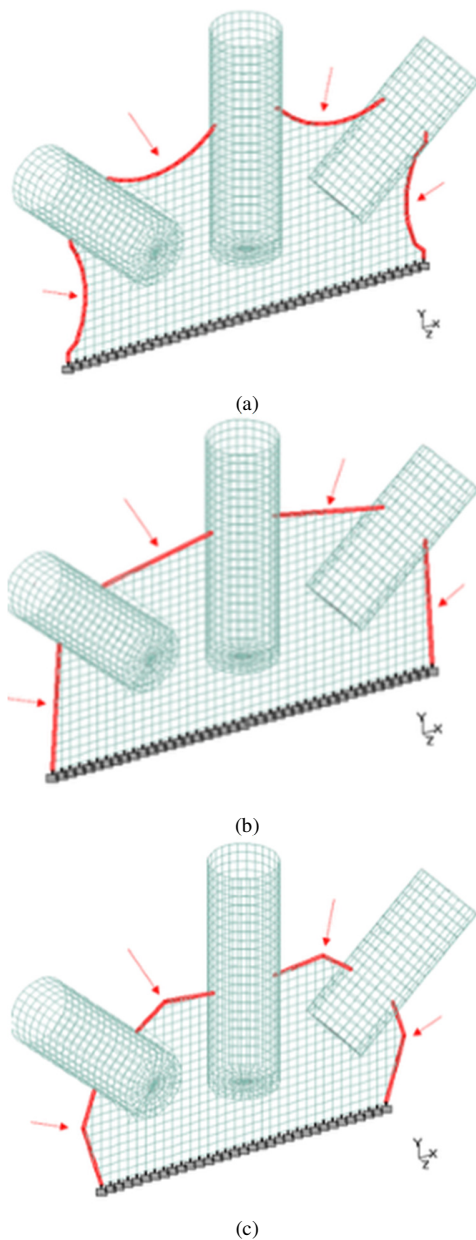


Fig. 2. Module support frame: (a) model 1 (Round), (b) model 2 (Flat), and (c) model 3 (Corner).

TABLE I. STEEL PROPERTIES

Property	Symbol	Value	Unit
Modulus of Elasticity	$E$	$2.06 \times 10^5$	MPa
Poisson's Ratio	$\nu$	0.3	-
Yield Strength	$\sigma_y$	355	MPa
Ultimate Strength	$\sigma_u$	490	MPa
Density	$\rho$	7850	kg/m <sup>3</sup>

The allowable stress is determined by:

$$\sigma_{allow} = \frac{\sigma_y}{\gamma_m} \tag{1}$$

where  $\sigma_{allow}$  is the allowable stress of the structural steel (MPa), used as the safety threshold for stress evaluation,  $\sigma_y$  is the yield strength of the material, and  $\gamma_m$  is the material partial safety factor, accounting for uncertainties related to material properties, fabrication tolerances, and modeling simplifications.

D. Meshing

In FEA, mesh refinement plays a crucial role in ensuring accurate stress prediction while maintaining computational efficiency. FEM-based analyses of industrial steel frameworks and heavy machinery structures provide an understanding of stress distribution, deformation, and dynamic behavior under various loading conditions. This approach enhances the theoretical framework by enabling the precise modeling of complex geometries and material properties, facilitating optimization and safety assessments [22, 23]. The mesh element sizes were varied from 30 mm, 40 mm, 50 mm, 60 mm, and 70 mm. Each meshing configuration was applied to the same gusset plate geometry and boundary conditions to ensure a consistent comparison.

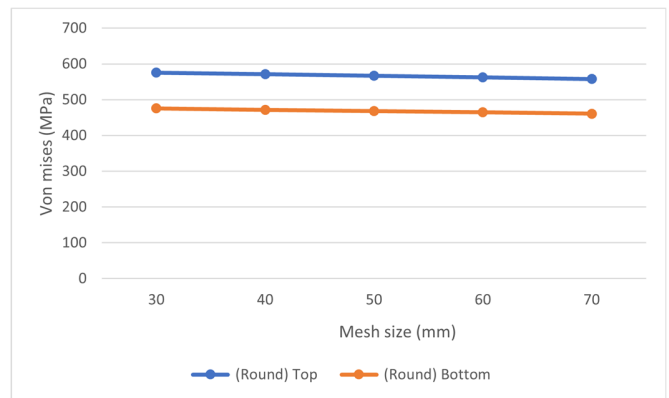


Fig. 3. Meshing convergence value (rough model).

As shown in Figure 3, the results indicate that the variation in the maximum Von Mises stress among the five mesh sizes was relatively small, with differences of less than 3%, indicating that mesh convergence had been achieved. Beyond an element size of 50 mm, further mesh refinement did not lead to a significant change in the stress results, while substantially increasing the computational cost. To ensure numerical reliability, the mesh convergence behavior was evaluated by comparing the peak stress responses for multiple mesh sizes. Based on this assessment, a uniform mesh size of 50 mm was used in all subsequent analyses. This mesh configuration provides sufficient resolution to accurately capture the stress gradients and concentration zones near the gusset plate connections while maintaining reasonable computational efficiency.

E. Loading and Boundary Conditions

External loads were applied through master nodes positioned at the top ends of the three column members, as depicted in Figure 4. Each master node (green cube) acts as a reference control point that distributes the applied forces and

moments to the corresponding slave nodes (purple nodes) along the column circumference using coupling constraints. This constraint formulation ensures uniform load transfer across the column cross-section, thereby providing a realistic representation of how axial forces and moments are transmitted to the gusset plate connection.

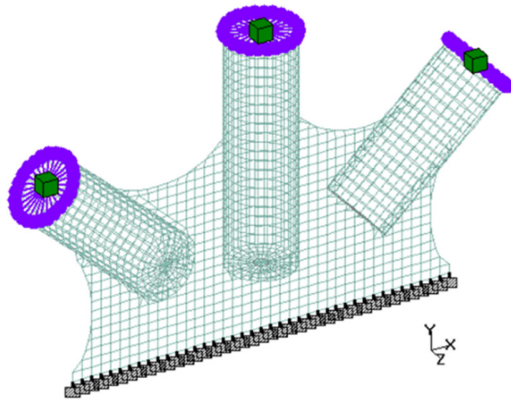


Fig. 4. Master and slave nodes in the model.

As presented in Figure 5, the loading configuration consisted of axial compressive forces acting along the longitudinal axes of the columns and rotational moments applied about the same axes. These conditions represent the combined effects of the operational and structural loads typically experienced by production module support structures.

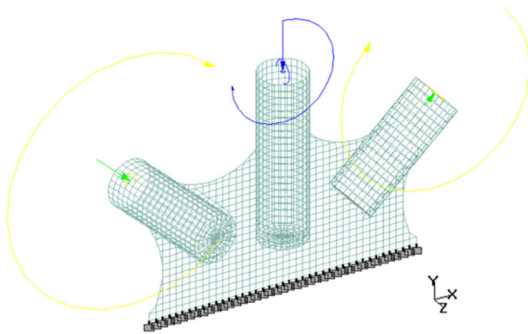


Fig. 5. Applied load in the model.

All three models were subjected to identical loading and boundary conditions to ensure consistency in the numerical evaluation. The only variation among the models was the geometry of the gusset plate, allowing a direct comparison of the influence of the plate configuration on the stress distribution and deformation behavior.

#### F. Finite Element Discretization

The gusset plate and adjacent members were discretized using quadrilateral shell elements. Mesh refinement was applied to regions expected to have high stress gradients (near the weld lines). The global stiffness equation is formulated as:

$$[K]\{u\} = \{F\} \quad (2)$$

where  $[K]$  is the stiffness matrix,  $\{u\}$  is the displacement vector, and  $\{F\}$  is the external force vector.

#### G. Stress Evaluation

The nodal and elemental stresses were extracted and compared among the three models. The equivalent von Mises stress is used as the primary failure criterion:

$$\sigma_{vm} = \sqrt{\sigma_x^2 + \sigma_y^2 - \sigma_x\sigma_y + 3\tau_{xy}^2} \quad (3)$$

where  $\sigma_{vm}$  is the Von Mises equivalent stress (MPa), representing a scalar measure of the multiaxial stress state,  $\sigma_x$  is the normal stress in the global or local x-direction (MPa),  $\sigma_y$  is the normal stress in the global or local y-direction (MPa), and  $\tau_{xy}$  is the in-plane shear stress acting on the xy-plane (MPa). These stress components are directly obtained from the finite element results at each integration point of the shell elements used to model the gusset plate.

### III. RESULTS AND DISCUSSION

The evaluation focuses on stress distribution, deformation behavior, and the comparison of maximum stress values among the models. The primary objective is to assess how variations in gusset geometry influence stress concentration under identical loading and boundary conditions. Figure 6 shows the Von Mises stress contours for the Flat, Corner, and Round gusset plate models. Although all configurations display a similar general stress distribution pattern, the highest stress concentrations occur near the welded connections between the gusset plate and the column members. However, the magnitude and spatial distribution of these stresses vary significantly depending on the gusset plate geometry.

In the Flat model, the stress concentration was localized and relatively low compared to the other two models. The Corner model exhibited the highest stress intensity, which spread across a larger region owing to the sharp corner geometry. The Round model showed a reduction in stress concentration, demonstrating the benefit of smoother transitions in the load path. The maximum Von Mises stress values obtained for each configuration at the top and bottom surfaces are summarized in Table III. These results provide a quantitative comparison of the stress magnitude and distribution across different gusset plate geometries.

The Corner model exhibited the highest Von Mises stress, exceeding the yield strength of AH/DH36 steel (355 MPa). The Flat model recorded the lowest stress level, whereas the Round model showed intermediate values. This indicates that the gusset geometry plays a significant role in reducing the stress concentration and improving the structural efficiency. Figure 7 compares the Von Mises stress values between the top and bottom surfaces for each model. The stress distribution trends were consistent between the two surfaces, with the top surface generally experiencing higher stresses owing to the applied loading direction and connection stiffness.

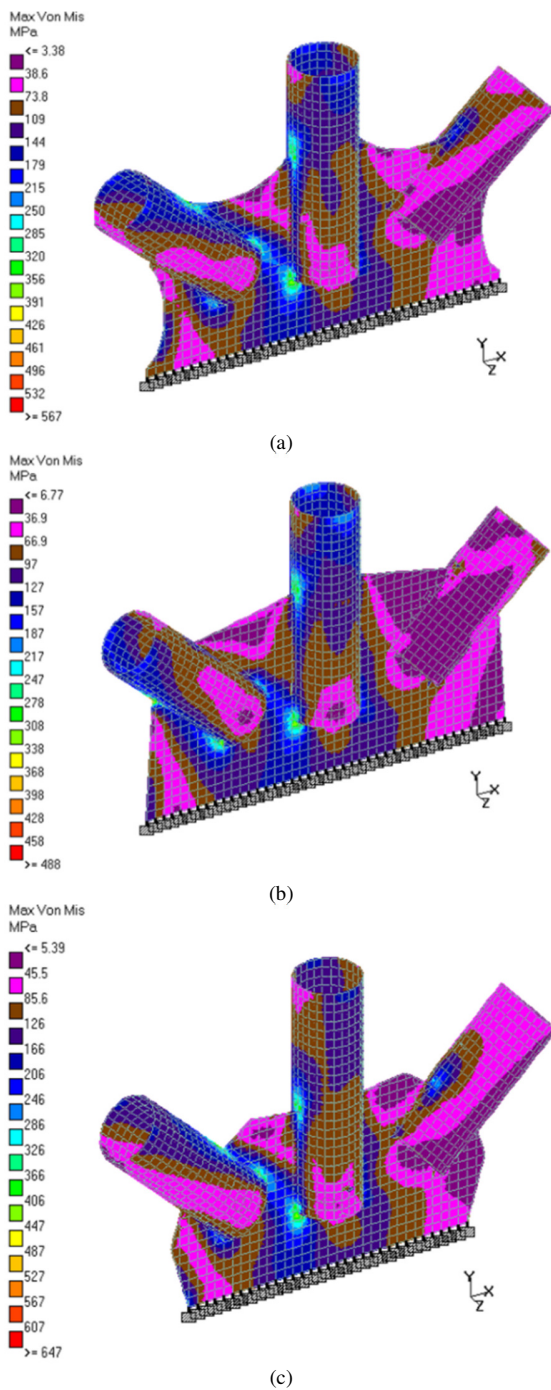


Fig. 6. Von Mises stress distribution: (a) model 1 (Round), (b) model 2 (Flat), (c) model 3 (Corner).

TABLE II. MAXIMUM VON MISES FOR EACH MODEL

Model Type	Top (MPa)	Bottom (MPa)	Description
Round gusset	566.839	468.242	Intermediate stress
Flat gusset	474.236	378.332	Lowest stress
Corner gusset	647.068	542.862	Highest stress

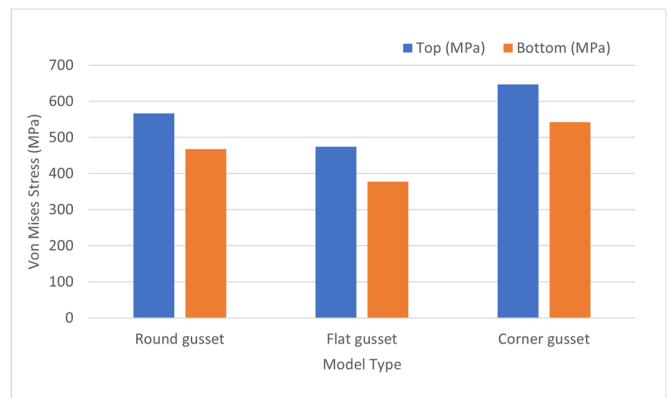


Fig. 7. Comparison of Von Mises stress between top and bottom surfaces for the three gusset plate models.

The Corner model exhibited the largest discrepancy between the top and bottom surface stresses, indicating non-uniform load transfer through the connection. In contrast, the Round model showed a more gradual stress variation, reflecting a smoother load path. The Flat model maintained the most uniform stress distribution between the two surfaces, suggesting improved load transfer efficiency across the gusset plate. The comparative results demonstrate that geometric modification significantly influences stress behavior. The Flat configuration provides superior structural performance by reducing stress concentration and maintaining lower stress magnitudes throughout the plate. Although the Corner configuration may enhance local rigidity, the presence of sharp geometric transitions generates excessive stress concentration, increasing the risk of localized yielding. Introducing rounded or filleted transitions, as implemented in the Round model, effectively mitigates stress concentration and improves the structural reliability of the module support connection.

#### IV. CONCLUSIONS

Gusset plates are crucial components in Floating Production Storage and Offloading (FPSO) topside module support structures, as they ensure effective load transfer and maintain joint stiffness. However, most existing studies emphasize global structural response, while the localized stress behavior of gusset plates has received comparatively limited attention. The present study addressed this gap by conducting a Finite Element Analysis (FEA) of three gusset plate geometries, Round, Flat, and Corner, under identical material properties, loading conditions, boundary constraints, and mesh convergence criteria. The results demonstrate that gusset geometry has a significant influence on stress concentration. The Corner model generated the highest Von Mises stress due to sharp geometric discontinuities, the Round model exhibited intermediate stress levels, and the Flat model consistently produced the lowest stress values with a more uniform distribution. The main contribution of this study lies in isolating the effect of gusset plate geometry on localized structural behavior within FPSO module supports. The findings provide evidence that geometric optimization alone can substantially improve joint performance and structural reliability. From a practical design perspective, the Flat gusset configuration is proposed as a safer and more efficient

alternative for production module support structures. The present analysis assumes linear elastic material behavior and simplified loading scenarios. Future research should incorporate nonlinear material models, more complex load combinations, and fatigue assessment to achieve a more comprehensive evaluation of structural robustness.

#### ACKNOWLEDGMENT

The authors would like to express their sincere gratitude to the Department of Naval Architecture, Faculty of Engineering, Hasanuddin University, for providing the computational facilities and academic support required to complete this study. The use of numerical analysis tools and guidance from the academic supervisors greatly contributed to the success of this study.

#### REFERENCES

- [1] U. Bhardwaj, A. P. Teixeira, C. Guedes Soares, A. K. Ariffin, and S. S. Singh, "Evidence based risk analysis of fire and explosion accident scenarios in FPSOs," *Reliability Engineering & System Safety*, vol. 215, Nov. 2021, Art. no. 107904, <https://doi.org/10.1016/j.ress.2021.107904>.
- [2] Y. Huang, Y. He, Y. Liu, M. Qiu, and M. Li, "Design and numerical simulation of the elastomeric support for the topside modules of an FPSO," *Ocean Engineering*, vol. 307, Sept. 2024, Art. no. 118203, <https://doi.org/10.1016/j.oceaneng.2024.118203>.
- [3] Y. Huang, Y. He, Y. Liu, M. Qiu, M. Li, and Z. Luo, "Application and analysis of elastomeric supporting style for topside modules of a spread mooring FPSO," *Ocean Engineering*, vol. 261, Oct. 2022, Art. no. 112183, <https://doi.org/10.1016/j.oceaneng.2022.112183>.
- [4] Y.-S. Shin and H.-J. Kim, "A comprehensive method for evaluating compressive strength and buckling behavior of corner gusset plates with various shapes," *Engineering Structures*, vol. 333, June 2025, Art. no. 120158, <https://doi.org/10.1016/j.engstruct.2025.120158>.
- [5] C. Wang, J. Yang, G. Li, T. Xie, K. Deng, and T. Xu, "Experimental study and analysis of UHPC-RC composite multi-column frame piers," *Structures*, vol. 82, Dec. 2025, Art. no. 110479, <https://doi.org/10.1016/j.istruc.2025.110479>.
- [6] G. A. Bisinotto, J. V. Sparano, A. N. Simos, F. G. Cozman, M. D. Ferreira, and E. A. Tannuri, "Sea state estimation based on the motion data of a moored FPSO using neural networks: An evaluation with multiple draft conditions," *Ocean Engineering*, vol. 276, May 2023, Art. no. 114235, <https://doi.org/10.1016/j.oceaneng.2023.114235>.
- [7] D.-S. Kwon, C. Jin, M. Kim, A. Guha, O. E. Esenkov, and S. Ryu, "Data-driven inverse estimation of ocean wave parameters using field-measured FPSO motion and environmental data," *Ocean Engineering*, vol. 341, Dec. 2025, Art. no. 122683, <https://doi.org/10.1016/j.oceaneng.2025.122683>.
- [8] M. Ghaderi-Garekani and S. Maleki, "Experimental and numerical investigations of block shear failure in gusset plates welded to double angle members," *Structures*, vol. 48, pp. 1356–1372, Feb. 2023, <https://doi.org/10.1016/j.istruc.2023.01.047>.
- [9] Y. Huang, Y. He, M. Qiu, Y. Liu, and M. Li, "Study of the wet-towing transportation of an FPSO with elastomeric-supporting topside modules," *Ocean Engineering*, vol. 293, Feb. 2024, Art. no. 116602, <https://doi.org/10.1016/j.oceaneng.2023.116602>.
- [10] S. D. Pham, A. Karamanli, N.-D. Nguyen, and T. P. Vo, "Vibration and buckling analysis of laminated and bio-inspired helicoidal composite curved beams," *Structures*, vol. 82, Dec. 2025, Art. no. 110480, <https://doi.org/10.1016/j.istruc.2025.110480>.
- [11] S. D. Dillen and C. Mittelstedt, "Efficient post-buckling analysis of laminated plates with bending–twisting coupling using a novel algorithmic implementation," *Composite Structures*, vol. 373, Dec. 2025, Art. no. 119646, <https://doi.org/10.1016/j.compstruct.2025.119646>.
- [12] A. Kohli, M. Mathad, S. V. Hosamani, M. K. Adagimath, and B. B. Kotturshettar, "Finite element analysis of knee joint implant for varying bio material using ANSYS," *Materials Today: Proceedings*, vol. 59, pp. 941–950, Jan. 2022, <https://doi.org/10.1016/j.matpr.2022.02.017>.
- [13] D. Y. Ali and R. A. Mahmood, "Influence of Slenderness Ratio and Sectional Geometry on the Behavior of Steel braced Frames," *Engineering, Technology & Applied Science Research*, vol. 14, no. 3, pp. 14282–14286, June 2024, <https://doi.org/10.48084/etasr.7314>.
- [14] T. Nguyen-Van and T. Bui-Tien, "Investigation of the Eigenvector of Stochastic Finite Element Methods of Functionally Graded Beams with Random Elastic Modulus," *Engineering, Technology & Applied Science Research*, vol. 13, no. 4, pp. 11253–11257, Aug. 2023, <https://doi.org/10.48084/etasr.5991>.
- [15] W. Wang *et al.*, "Interfacial bonding stress transfer and failure mechanism between corrugated steel plate and reinforced concrete," *Engineering Failure Analysis*, vol. 153, Nov. 2023, Art. no. 107555, <https://doi.org/10.1016/j.engfailanal.2023.107555>.
- [16] J. Xie and W. Zhang, "Numerical analysis on steel bracing members with bolted gusset plate connections," *Journal of Constructional Steel Research*, vol. 222, Nov. 2024, Art. no. 108960, <https://doi.org/10.1016/j.jcsr.2024.108960>.
- [17] Y.-S. Shin and H.-J. Kim, "Net-section fracture resistances of bolted gusset plates with various connection details," *Journal of Constructional Steel Research*, vol. 227, Apr. 2025, Art. no. 109350, <https://doi.org/10.1016/j.jcsr.2025.109350>.
- [18] Y. Cao, Y. Zhou, G. Zhong, and K. Jiang, "Structural performance of cruciform butted connected gusset plates under tensile loading," *Journal of Constructional Steel Research*, vol. 235, Dec. 2025, Art. no. 109934, <https://doi.org/10.1016/j.jcsr.2025.109934>.
- [19] Y. Zarei, A. Afsari, S. M. R. Nazemosadat, and M. Mohammadi, "Simulation and Thermo-Mechanical Analysis of AA6063-T5 in FSW by FEM," *Journal of Modern Processes in Manufacturing and Production*, vol. 2, no. 2, Sept. 2024, Art. no. 5, <https://doi.org/10.71762/d5yp-e678>.
- [20] M. Mohammadi, S. M. R. Nazemosadat, D. Fazel, and Y. Bazargan Lari, "An integrated approach for structural modeling, modal analysis, and aerodynamic evaluation of an electric vehicle body shell using finite element method and computational fluid dynamics," *Materials Today Communications*, vol. 45, Apr. 2025, Art. no. 112331, <https://doi.org/10.1016/j.mtcomm.2025.112331>.
- [21] S. M. R. Nazemosadat, D. Ghanbarian, M. Naderi-Boldaji, and M. A. Nematollahi, "Structural analysis of a mounted moldboard plow using the finite element simulation method," *Spanish Journal of Agricultural Research*, vol. 20, no. 2, pp. e0204–e0204, Mar. 2022, <https://doi.org/10.5424/sjar/2022202-18157>.
- [22] M. Mohammadi, S. M. R. Nazemosadat, and A. Afsari, "Modeling and Analysis of a Tractor Diesel Engine Test Stand Structure Using the Finite Element Method," *Biomechanism and Bioenergy Research*, vol. 3, no. 2, pp. 75–87, Dec. 2024, <https://doi.org/10.22103/bbr.2024.24161.1090>.